JACS
JOURNAL OF THE AMERICAN CHEMICAL SOCIETY

ARTICLE

pubs.acs.org/JACS

Sensitive and Selective Chromogenic Sensing of Carbon Monoxide via Reversible Axial CO Coordination in Binuclear Rhodium Complexes

María E. Moragues,[†,‡,§] Julio Esteban,[†,‡] José Vicente Ros-Lis,[†,‡] Ramón Martínez-Máñez,[*,†,‡,§] M. Dolores Marcos,[†,‡,§] Manuel Martínez,[*,∥] Juan Soto,[†,‡] and Félix Sancenón[†,‡,§]

[†]Centro de Reconocimiento Molecular y Desarrollo Tecnológico (IDM), Unidad Mixta Universidad Politécnica de Valencia-Universidad de Valencia, Spain

[‡]Departamento de Química, Universidad Politécnica de Valencia, Camino de Vera s/n, E-46022 Valencia, Spain

[§]CIBER de Bioingeniería, Biomateriales y Nanomedicina (CIBER-BBN)

[∥]Departament de Química Inorgànica, Universitat de Barcelona, Martí i Franquès 1-11, E-08028 Barcelona, Spain

Supporting Information

ABSTRACT: The study of probes for CO sensing of a family of binuclear rhodium(II) compounds of general formula $[Rh_2\{(XC_6H_3)P(XC_6H_4)\}_n(O_2CR)_{4-n}]\cdot L_2$ containing one or two metalated phosphines (in a head-to-tail arrangement) and different axial ligands has been conducted. Chloroform solutions of these complexes underwent rapid color change, from purple to yellow, when air samples containing CO were bubbled through them. The binuclear rhodium complexes were also adsorbed on silica and used as colorimetric probes for "naked eye" CO detection in the gas phase. When the gray-purple colored silica solids containing the rhodium probes were exposed to air containing increasing concentrations of CO, two colors were observed, in agreement with the formation of two different products. The results are consistent with an axial coordination of the CO molecule in one axial position (pink-orange) or in both (yellow). The crystal structure of **3·(CO)** ($[Rh_2\{(C_6H_4)P(C_6H_5)_2\}_2(O_2CCF_3)_2]\cdot CO$) was solved by single X-ray diffraction techniques. In all cases, the binuclear rhodium complexes studied showed a high selective response to CO with a remarkable low detection limit. For instance, compound **5·$(CH_3CO_2H)_2$** ($[Rh_2\{(m\text{-}CH_3C_6H_3)P(m\text{-}CH_3C_6H_4)_2\}_2(O_2CCH_3)_2]\cdot(CH_3CO_2H)_2$) is capable of detection of CO to the "naked eye" at concentrations as low as 0.2 ppm in air. Furthermore, the binding of CO in these rhodium complexes was found to be fully reversible, and release studies of carbon monoxide via thermogravimetric measurements have also been carried out. The importance of the silica support for the maintenance of the CO-displaced L ligands in the vicinity of the probes in a noninnocent manner has been also proved.

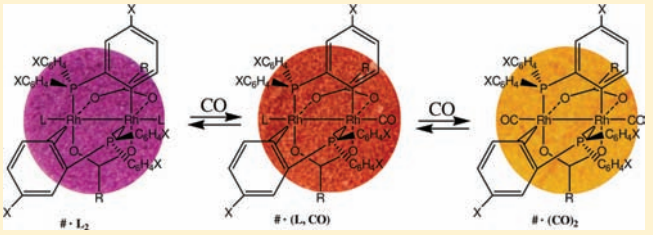

INTRODUCTION

Carbon monoxide is an airborne contaminant difficult to detect since it is colorless and odorless and toxic at low concentration levels. Moreover, this compound may present a real danger to humans[1] in automobiles, airplanes, industrial plants, mines, homes, and other environments in which persons may be present for extended periods of time. Typical anthropogenic sources of this deadly pollutant involve combustion engines and improper burning of other fuels. Examples include residential furnaces, gasoline engines, charcoal grills, gas heaters, and others. Carbon monoxide toxicity lies in the fact that hemoglobin presents about 200 times higher affinity for carbon monoxide than for oxygen. Therefore, carbon monoxide can readily displace oxygen on hemoglobin,[2] reducing the amount of the latter that can be carried to tissues and impairing the mechanisms of cellular respiration.[3] For this reason, carbon monoxide is toxic to humans at relatively low concentrations.[4] For healthy adults, CO becomes toxic when it reaches a level higher than 50 ppm with continuous exposure over an eight hour period. Mild exposure over a few hours (a CO level between 70 and 100 ppm) includes flu-like symptoms, such as headaches, sore eyes, and a runny nose. Medium exposure (a CO level between 150 and 300 ppm) will produce dizziness, drowsiness, and vomiting. Extreme exposure (a CO level of 400 ppm and higher) will result in unconsciousness, brain damage, and death. Unfortunately, it is quite usual that people with CO poisoning overlook the symptoms (e.g., headache, nausea, dizziness, or confusion), and unintentional CO exposure accounts for an estimated 15 000 emergency department visits and 500 unintentional deaths in the United States alone each year.

Therefore, there is an increasing interest for the development of chemical sensor systems capable of detecting the presence of carbon monoxide in air at low concentrations. Most existing CO sensors use metal-oxide semiconductors (MOS)[5] that have been widely chosen as gas-sensing devices and applied in monitoring

Received: July 20, 2011
Published: August 24, 2011

   dx.doi.org/10.1021/ja206251r | J. Am. Chem. Soc. 2011, 133, 15762–15772

quality air control. As an alternative to these methods, the development of chromogenic sensing systems for CO detection at poisonous concentrations is of great importance. Colorimetric methods are especially undemanding offering several advantages over other analytical procedures, such as real-time monitoring and the use of very simple and inexpensive instrumentation. Additionally, certain colorimetric changes, even at low concentration of analytes, can be observed to the "naked eye", thus making chromogenic protocols unbeatable for certain applications.

However, colorimetric probes for the detection of this deadly chemical are still rare. An example involves the use of oxoacetato-bridged triruthenium cluster complexes,[6] which show color changes in acetonitrile. An electron transfer process with a zinc tetraphenylporphyrin changes the oxidation state of the ruthenium metal center thus allowing its coordination to carbon monoxide. Polypyrrole functionalized with iron porphyrin has also been reported to act as a suitable material for carbon monoxide detection at low concentrations in water/methanol solutions.[7] In a recent example, a stereospecific binding of CO at a pentacoordinated diisopropylphosphino diaminopyridine iron complex when exposed to high concentrations of carbon monoxide (1 atm of gaseous CO) has been reported; the corresponding hexacoordinated derivative is formed, as indicated by the color change from yellow to red.[8] The optical detection of parts-per-million levels of carbon monoxide in air by UV−vis spectroscopy in the transmission mode using a monolayer of bimetallic rhodium complexes has also been reported, although with relatively poor changes in color.[9] In all reported examples, until now, the modulations in the presence of carbon monoxide show certain shortcomings typically involving poor color changes. Additionally, in most cases colorimetric CO detection was performed in solution but not in air. Furthermore, relatively large detection limits hamper their use as reliable sensing systems.

Following our interest in the design of novel chromogenic systems,[10] we considered the application of binuclear rhodium compounds as potential colorimetric probes for the sensing of CO by exploiting the well-known ability of these complexes to coordinate different bases in their labile axial sites.[11] In a recent preliminary communication,[12] we have reported the development of a colorimetric probe based on the binuclear rhodium compound $\mathbf{2\cdot(CH_3CO_2H)_2}$ of formula $[Rh_2\{(C_6H_4)P(C_6H_4)_2\}_2(O_2CCH_3)_2]\cdot(CH_3CO_2H)_2$. On the basis of the excellent sensing results obtained for this rhodium complex in terms of selectivity and sensitivity, we report herein an extended study using a family of binuclear rhodium(II) complexes of general formula $[Rh_2\{(XC_6H_3)P(XC_6H_4)_2\}_n(O_2CR)_{4-n}]\cdot L_2$ containing one or two (in a head-to-tail arrangement) metalated phosphine ligands and different axial ligands. For these compounds, the color modulations observed in the presence of carbon monoxide, and induced via axial labile coordination of CO groups, have been studied.

RESULTS AND DISCUSSION

Design of the Probe Complexes. The design of the chromogenic probes involves the use of binuclear rhodium(II) cyclometalated complexes and the well-documented labile coordination ability of these compounds in their axial sites. These have been demonstrated to act both in their own reactivity[13,14] and as catalytic centers[15] in a number of transformations.[16] Additionally, some coordination studies on adduct formation between dirhodium compounds and different Lewis bases[11] have pointed out that even relatively simple systems such as tetra-μ-carboxylate-dirhodium(II) derivatives show an important π-back-bonding capability of the rhodium(II) atoms. This fact has been attributed to an extensive mixing of the orbitals with π symmetry on the two metal centers. This effect causes the rhodium(II) metal centers to be very effective in π-back-bonding to the axial ligands which is a very interesting feature for the design of CO binding complexes.[17] In addition, when biscyclometalated compounds are compared with dirhodium tetracarboxylate derivatives, a higher ability of the former for π-back-donation to the axial ligand has been reported. Moreover, it has been observed, in much of the chemistry associated with dirhodium(II) cyclometalated complexes, that the presence of different ligands coordinated to the axial positions of these derivatives produce important changes in the UV−vis spectra in solution.[18,19]

These enhanced π-back-donation properties of dirhodium(II) cyclometalated complexes and the color changes observed upon axial coordination with different ligands make these complexes suitable as potential chromogenic systems for CO detection. With these design concepts in mind, we have recently reported a colorimetric probe based on a binuclear cyclometalated rhodium compound. On the basis of the possible modulation of the sensing features via changes in the donor−acceptor properties of the π-bringing ligands, we have prepared a family of binuclear rhodium complexes (see Scheme 1) of general formula[20] $[Rh_2\{(XC_6H_3)P(XC_6H_4)_2\}_n(O_2CR)_{4-n}]\cdot L_2$ containing one (n = 1) or two (n = 2) metalated phosphine ligands[21] in a head-to-tail arrangement. Two different phosphines (X = H or m-CH_3) and three different carboxylic acids (R = CH_3, CF_3, or $C(CH_3)_3$) as equatorial ligands, as well as four different axial ligands (L = CH_3CO_2H, CF_3CO_2H, $(CH_3)_3CCO_2H$, or H_2O),

Scheme 1. General Structure for Binuclear Rhodium Compounds Used in This Work

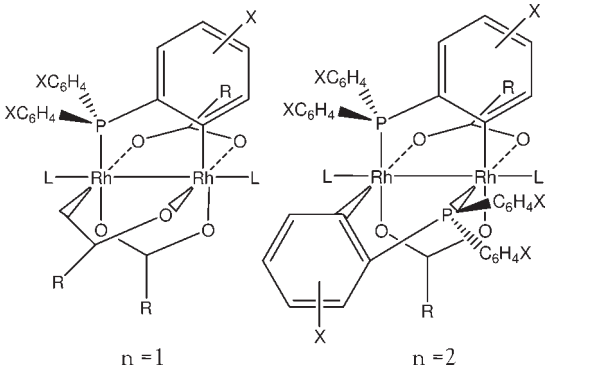

Table 1. Binuclear Rhodium Compounds Used in This Work with General Formula $[Rh_2\{(XC_6H_3)P(XC_6H_4)_2\}_n(O_2CR)_{4-n}]\cdot L_2$

compound	n	X	R	L
$\mathbf{1\cdot(CH_3CO_2H)_2}$	1	H	CH_3	CH_3CO_2H
$\mathbf{2\cdot(CH_3CO_2H)_2}$	2	H	CH_3	CH_3CO_2H
$\mathbf{2\cdot(H_2O)_2}$	2	H	CH_3	H_2O
$\mathbf{3\cdot(CF_3CO_2H)_2}$	2	H	CF_3	CF_3CO_2H
$\mathbf{4\cdot((CH_3)_3CCO_2H)_2}$	2	H	$C(CH_3)_3$	$(CH_3)_3CCO_2H$
$\mathbf{5\cdot(CH_3CO_2H)_2}$	2	m-CH_3	CH_3	CH_3CO_2H

dx.doi.org/10.1021/ja206251r |J. Am. Chem. Soc. 2011, 133, 15762–15772

Scheme 2. Complexes with General Structure $[Rh_2\{(XC_6H_3)P(XC_6H_4)_2\}_n(O_2CR)_{4-n}]\cdot L_2$, Simplified as $\#\cdot L_2$, and the Corresponding Products, Simplified as $\#\cdot(L,CO)$ and $\#\cdot(CO)_2$, Obtained upon Coordination of Carbon Monoxide at Labile Axial Positions

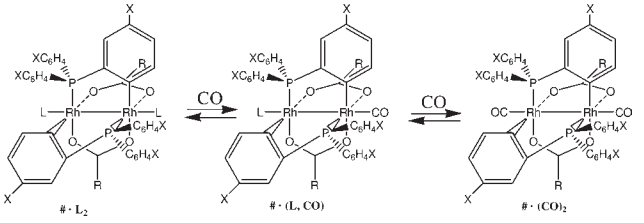

have been used. Table 1 shows the different compounds studied.

Reactivity with Carbon Monoxide. Once the family of birhodium derivatives was prepared, UV−vis spectrophotometric studies for the CO coordination of all compounds, i.e., $\mathbf{1\cdot(CH_3CO_2H)_2}$, $\mathbf{2\cdot(CH_3CO_2H)_2}$, $\mathbf{2\cdot(H_2O)_2}$, $\mathbf{3\cdot(CF_3CO_2H)_2}$, $\mathbf{4\cdot((CH_3)_3CCO_2H)_2}$, and $\mathbf{5\cdot(CH_3CO_2H)_2}$, were carried out in chloroform solution. All complexes, $\mathbf{\#\cdot L_2}$, underwent a fast and distinct color change, from purple to yellow, when CO-containing air samples were bubbled through their chloroform solutions. Furthermore, depending on the concentration of CO in the air samples, two different products were obtained, with two distinct electronic spectra. For low CO concentrations, the purple solutions turned pink-orange, whereas at high CO concentration solutions became yellow. Interestingly, when CO-free air was bubbled on these final yellow solutions, the color reverted to purple, thus indicating that the process is reversible. All these observations agree with the formation of the corresponding mono-, $\mathbf{\#\cdot(L,CO)}$, and bis-CO-substituted, $\mathbf{\#\cdot(CO)_2}$, species (Scheme 2) of the dirhodium(II) starting materials.

Characterization of the Axial Carbon Monoxide Complexes. The crystal structures of dirhodium complexes containing cyclometalated phosphines have already been extensively reported.[20,22,23] All the molecular structures of dirhodium(II) complexes **2**−**5** are very similar and can be rationalized with the single scheme in Figure 1a. All of them contain two bonded rhodium atoms that are also bridged by two carboxylate groups and two phosphine ligands. In the latter, metalation has occurred at one of the phenyl rings of each, producing a head-to-tail final conformation. Compound $\mathbf{1\cdot(CH_3CO_2H)_2}$ is a little bit different as it contains three carboxylates and one phosphine ligand bridging the dirhodium(II) lantern core. Additionally, the coordination spheres of the metal atoms are completed by means of two other ligands, mainly acetic acid and trifluoroacetic acid, that occupy the labile axial positions. In this way, a slightly distorted octahedral coordination exists around each of the metal atoms in the dirhodium(II) group. The values of the Rh−Rh bond distances in these bismetalated complexes present a very small variation (in the 2.499(2)−2.513(2) Å range), whereas a slightly shorter distance, 2.430(2) Å, is found for the monometalated analog. The d_{Rh-P} and d_{Rh-C} bond distances represent a wider range (2.193(6)−2.220(3) Å and 1.960(2)−2.020(2) Å, respectively), while the variation in the Rh−O_{axial} distances (2.301(4)−2.412(5) Å) represents the largest margin. It is interesting to note that the d_{Rh-L} and d_{Rh-Rh} bond distances do not show any significant trend upon variation of either the carboxylate R or the axial L groups, apart from that derived from the inherent steric

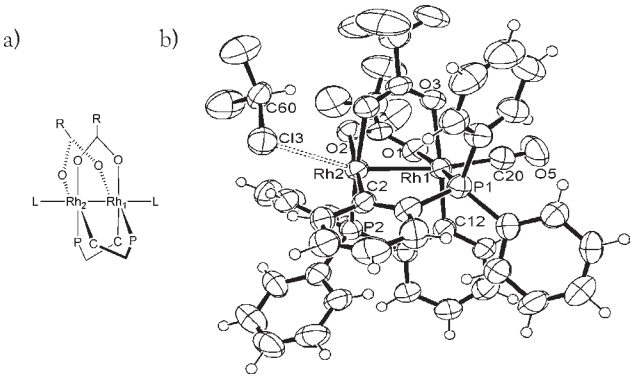

Figure 1. (a) Simplified scheme of the structures of compounds $\mathbf{2\cdot L_2}$ to $\mathbf{5\cdot L_2}$. (b) ORTEP plot of the crystal structure of $\mathbf{3\cdot(CHCl_3,CO)}$; thermal ellipsoids are set at the 50% probability level. Selected bond lengths [Å] and angles [°]: Rh1−Rh2, 2.5333(9); Rh1−P1, 2.2574(23); Rh1−C20, 1.9698(122); Rh2−P2, 2.2132 (21); Rh2−Cl3, 2.9023(31); C20−O5, 1.1042(152); Rh1−C20−O5, 176.63(1).

hindrance caused by the more bulky groups. In this respect, the observed Rh−Rh−O_{axial} bond angles in the monometalated complex **1**, 169.0(1)° and 174.4(1)°, deviate only slightly from linearity, while for the doubly metalated complexes deviations are more significant (within the 163.6(1)−166.9(1)° range).

To understand the ability of carbon monoxide to bind these dirhodium complexes in the axial positions, the comparison between the previously reported structures and those of the corresponding CO-substituted complexes should be conducted. Suitable crystals for single X-ray diffraction were obtained by slow evaporation of CO-bubbled chloroform solutions of the desired compounds layered with hexane. The crystal structures of two different families of compounds have been obtained: the first one (reported in a recent communication) is a mixture of $\mathbf{2\cdot(CH_3CO_2H,CO)}$ and $\mathbf{2\cdot(CO)_2}$,[12] while the second one, reported in this paper, corresponds to a $\mathbf{3\cdot(CHCl_3,CO)}$ stoichiometry.[24]

The molecular structure of compound $\mathbf{3\cdot(CHCl_3,CO)}$ (Figure 1b) consists of a rhodium binuclear core with two metalated phosphine ligands in a head-to-tail conformation and two carboxylate (trifluoroacetate) ligands in the equatorial positions, as expected by comparison with the **2** to **5** family of complexes. In this case, however, the coordination on the axial labile positions of the rhodium(II) centers is completed with only one carbon monoxide molecule ligand at a bonding distance. The second axial position is occupied by a solvent molecule (chloroform) at a very long distance (2.902(3) Å). Relevant crystallographic data are collected in Tables S1 and S2 (Supporting Information).

The structure reported here, together with the one recently reported,[12] allows the comparison of the series of analogous $[Rh_2\{(C_6H_4)P(C_6H_5)_2\}_2(O_2CR)_2]$ compounds differing only in the bridging carboxylate ligands (R = CH_3 or R = CF_3). Tables 2 and 3 collect the main metal−ligand distances and angles that allow a proper comparison between the two sets of data. The difference in the d_{Rh-Rh} bond lengths when the R groups of the carboxylate ligands change from CH_3 to CF_3 is rather small, 0.009 Å, as has already been found for all **2**−**5** known complexes (0.005 Å between $\mathbf{2\cdot(CH_3CO_2H)_2}$ and $\mathbf{3\cdot(CF_3CO_2H)_2}$). It is clear that the important change in the electronic character of these carboxylates has only a small influence

Table 2. Relevant Bond Distances (Å) for Biscyclometalated Binuclear Rhodium Compounds Used in This Work[a]

	$2\cdot(CH_3CO_2H)_2$[20]	$2\cdot(CH_3CO_2H,CO)$[12]	$3\cdot(CF_3CO_2H)_2$[26]	$3\cdot(CHCl_3,CO)$[b]
$d_{Rh1-Rh2}$	2.508(1)	2.5425(5)	2.513(2)	2.5333(9)
$d_{Rh1-Oax}$	2.342(5)	-	2.340(2)	-
$d_{Rh1-COax}$	-	1.9810(5)	-	1.9698(122)
$d_{Rh2-Oax}$	2.342(5)	2.3580(18)	2.360(14)	-
$d_{Rh2-COax}$	-	-	-	-
$d_{Rh1-Oav}$	2.190(4)	2.1520(3)	2.210(2)	2.1832(54)
$d_{Rh2-Oav}$	2.136(4)	2.1525(3)	2.210(2)	2.16765(7)
d_{Rh1-P}	2.210(2)	2.2384(12)	2.218(7)	2.2574(23)
d_{Rh2-P}	2.210(1)	2.2117(11)	2.205(7)	2.2132(21)
d_{Rh1-C}	1.997(4)	2.0400(4)	2.020(2)	2.0326(79)
d_{Rh2-C}	1.996(6)	2.0220(5)	1.990(2)	1.9942(82)

[a] Atom labeling corresponds to the nomenclature shown in Figure 1b. [b] Present work.

Table 3. Rh−Rh−L Angles (°) for Biscyclometalated Binuclear Rhodium Compounds Used in This Work

	$2\cdot(CH_3CO_2H)_2$	$2\cdot(CH_3CO_2H,CO)$	$3\cdot(CF_3CO_2H)_2$	$3\cdot(CHCl_3,CO)$
Rh_2-Rh_1-L	163.6(1)	171.03(14)	166.5(4)	170.71(33)
$L-Rh_2-Rh_1$	163.6(1)	167.40(4)	166.3(4)	-

on the intermetallic distance. A more important effect is found when the carboxylic acid in the axial positions is substituted by a carbon monoxide. In this case, the differences found are 1 order of magnitude larger (0.0345 Å between $\mathbf{2\cdot(CH_3CO_2H)_2}$ and $\mathbf{2\cdot(CH_3CO_2H,\ CO)}$; 0.0203 Å between $\mathbf{3\cdot(CF_3CO_2H)_2}$ and $\mathbf{3\cdot(CHCl_3,CO)}$). This effect fits very nicely with the π-acceptor character of the carbon monoxide molecule that withdraws electron density from the metal−metal bond. A combination of the two above-mentioned facts may be the actual reason for the high asymmetry of the $\mathbf{3\cdot(CHCl_3,CO)}$ complex. The complete coordination of the dirhodium(II) core in this complex can be achieved with only a simple solvent molecule, which supports the idea that the metal to axial ligand bond could not only be explained considering a pure sigma interaction.[11]

Having a look at the Rh-equatorial ligand distances, a similar trend is evident. A longer d_{Rh-P} distance is, nevertheless, observed for metal atoms having carbon monoxide in their coordination sphere, which is balanced by a shortening in the corresponding $d_{Rh\text{-}Oeq}$ bond lengths. Very similar averaged equatorial distances when changing the carboxylic acid by carbon monoxide are found in all cases.

With respect to the bond angles, a general deviation of linearity of the Rh−Rh−L unit, both for R = CH_3 and CF_3 (Table 3), is observed, probably due to the presence of the phosphine ligands in complexes $\mathbf{2\cdot(CH_3CO_2H,CO)}$ and $\mathbf{3\cdot(CHCl_3,CO)}$. The substitution of axial carboxylic acid molecules by carbon monoxide allows a relaxation in the Rh_2-Rh_1-L angles, producing less strained units.

Carbon Monoxide Sensing Behavior in Air. Despite the interesting spectrophotometric response of the studied dirhodium(II) complexes found in chloroform solutions, the detection of CO is of main importance in the gas phase. Therefore, we took a step forward toward the potential use of this kind of sensing derivatives as probes for the detection of carbon monoxide in air. Adsorption of compounds **1**−**5** on silica beads (via solution of each binuclear rhodium compound in a minimum amount of chloroform followed by the addition of silica at a weight ratio 2−10 times) resulted in purple solids. The solids were separated after five minutes of stirring at room temperature, and the solvent was removed on a rotary evaporator. The resulting solid was dried at 343 K for at least 48 h before use.

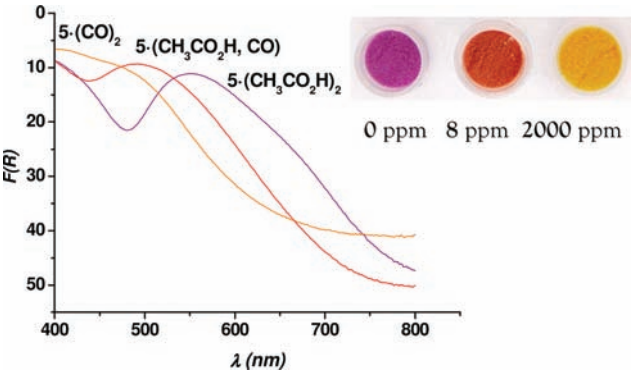

Figure 2. Diffuse reflectance UV−vis spectra of a mixture of silica containing $\mathbf{5\cdot(CH_3CO_2H)_2}$ and the changes observed in the presence of air containing 8 and 2000 ppm of CO.

The colored silica supports containing the rhodium probes underwent important color changes in seconds when exposed to air containing different concentrations of carbon monoxide. As observed in chloroform solutions, a more detailed study of the titration process, using increasing concentrations of carbon monoxide, clearly revealed that two consecutive substitution reactions occur. As an example, Figure 2 shows the diffuse reflectance UV−vis spectra of silica beads containing $\mathbf{5\cdot(CH_3CO_2H)_2}$ and the changes observed in the presence of air containing 8 and 2000 ppm of CO. Whereas $\mathbf{5\cdot(CH_3CO_2H)_2}$ shows a band at 550 nm, a large excess of CO (2000 ppm) resulted in the appearance of a new band at 412 nm, whereas at lower concentrations of CO (8 ppm) a band at 495 nm was observed. These changes are consistent with an axial coordination by CO and the formation of the derivatives $\mathbf{5\cdot(CO)_2}$ and $\mathbf{5\cdot(CH_3CO_2H,\ CO)}$ (Scheme 2).

Table 4. UV−vis Spectral Data for the Different Binuclear Rhodium(II) Compounds Studied in Chloroform Solution, As Well As Their Diffuse Reflectance Spectra Supported on Silica Beads, At Room Temperature[a]

	$CHCl_3$ solution	solid	
compound	λ_{max} (nm), (ε (M^{-1} cm^{-1}))	λ_{max} (nm)	ν_{CO} (cm^{-1})
$\mathbf{1}\cdot(CH_3CO_2H)_2$	556, (157)	550	
$\mathbf{1}\cdot(CO)_2$	394, (421)	400	2040
$\mathbf{2}\cdot(CH_3CO_2H)_2$	567, (552)	545	
$\mathbf{2}\cdot(CO)_2$	398, (7040)	398	2028
$\mathbf{3}\cdot(CF_3CO_2H)_2$	571, (711)	537	
$\mathbf{3}\cdot(CO)_2$	400, (6570)	402	2048
$\mathbf{4}\cdot(CH_3CO_2H)_2$	547, (560)	539	
$\mathbf{4}\cdot(CO)_2$	397, (3689)	400	2033
$\mathbf{5}\cdot(CH_3CO_2H)_2$	564, (265)	550	
$\mathbf{5}\cdot(CO)_2$	397, (1247)	412	2033

[a] The bands assigned to the CO stretch in the IR spectrum are also included.

Table 5. Detection Limits (ppm) for Compounds $\#\cdot L_2$ in the Presence of CO[a]

	detection limits (ppm) of CO	
compound	UV−vis spectrophotometer	naked eye
$\mathbf{1}\cdot(CH_3CO_2H)_2$	0.7	52
$\mathbf{2}\cdot(CH_3CO_2H)_2$	0.6	42
$\mathbf{2}\cdot(H_2O)_2$	1.6	35
$\mathbf{3}\cdot(CF_3CO_2H)_2$	0.8	38
$\mathbf{4}\cdot((CH_3)_3CCO_2H)_2$	1.7	50
$\mathbf{5}\cdot(CH_3CO_2H)_2$	<0.1	0.2

[a] Limits calculated from UV−visible spectral data (first column) and the to the naked eye (second column).

A very similar change in color and hypsochromic shift of the band was observed for all dirhodium(II) complexes studied. Table 4 shows the spectroscopic characteristics of the complexes in chloroform solutions, as well as adsorbed on silica, together with the data in the presence of an excess of carbon monoxide. Compounds **1**−**5** display an absorption band in the 550−570 nm range in chloroform that is not basically modified when adsorbed on silica beads. Upon addition of an excess of carbon monoxide, new bands centered in the 394−400 nm region were found for all complexes both in chloroform and on silica. The table also shows that the molar absorptivities of the corresponding carbon monoxide complexes are in general 1 order of magnitude larger than those of the starting derivatives.

Table 4 also collects the carbon monoxide stretching frequency for the $\#\cdot(CO)_2$ derivatives adsorbed on silica, which range from 2028 to 2048 cm^{-1}. These stretching ν_{CO} frequencies[25] are, in all cases, considerably lower than the CO stretching frequency of the free carbon monoxide (2143 cm^{-1}), which indicates the presence of highly acidic axial metal sites with relatively high levels of M → CO π-back-bonding. This effect is naturally stronger when donor groups are also present in the bridging carboxylate groups.

Perhaps one of the most remarkable behaviors in relation to the response of the tested dirhodium(II) complexes is that the chromogenic response is observed at relatively low concentrations of carbon monoxide. Titration studies of the derivatives **1**−**5** adsorbed on silica gel with increasing quantities of carbon monoxide in air allowed determining the detection limits for CO. From a chemosensing point of view, a low detection limit for carbon monoxide of less than 1.7 ppm was found for all studied complexes using a conventional UV−vis spectrophotometer (see Table 5). Figure 3 shows the changes in absorbance of the band centered at 557 nm of $\mathbf{5}\cdot(CH_3CO_2H)_2$ adsorbed on silica beads in the presence of different concentrations of CO in air; the response of complex $\mathbf{5}\cdot(CH_3CO_2H)_2$ to CO shows a lineal trend between 1 and 100 ppm at this wavelength. A similar lineal behavior was also found for the other rhodium derivatives studied.

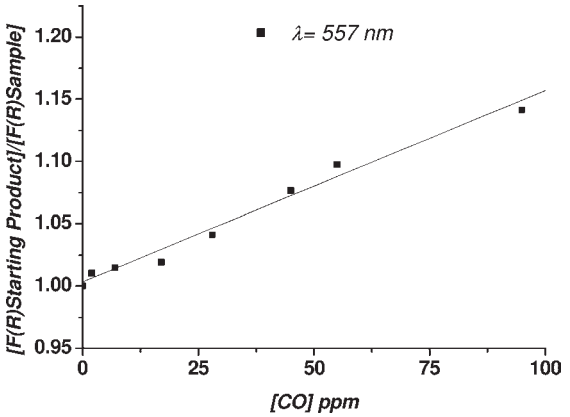

Figure 3. Loss of the intensity of the band centered at 557 nm vs concentration of CO in air for $\mathbf{5}\cdot(CH_3CO_2H)_2$ adsorbed on silica.

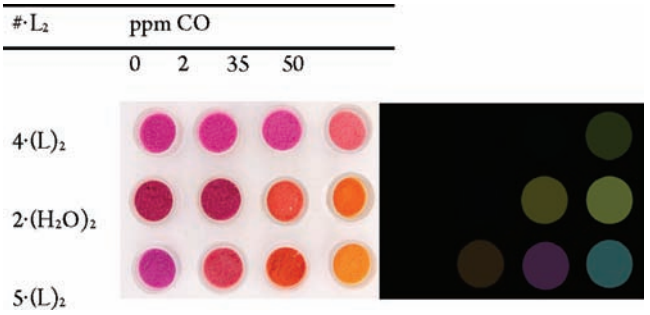

Figure 4. Sensing array of the studied complexes for CO detection in air. On the right, the increment of the RGB values is shown.

Table 5 indicates the estimated detection limit to the "naked eye" for compounds **1**−**5** in the presence of CO, i.e., the minimum amount of CO necessary to observe a clear color change in the complexes. All the compounds display a chromogenic modulation to the naked eye at concentrations at which CO is toxic (i.e., 50−60 ppm), and compound $\mathbf{5}\cdot(CH_3CO_2H)_2$ even shows a very remarkable color modulation at CO concentrations as low as 0.2 ppm.

This range of visual CO detection values found for all compounds made it possible to design systems for semiquantitative sensing of CO in air at different concentration ranges. For instance, a sensing array containing compounds $\mathbf{4}\cdot((CH_3)_3CCO_2H)_2$, $\mathbf{2}\cdot(H_2O)_2$, and $\mathbf{5}\cdot(CH_3CO_2H)_2$, displaying clear visual detection limits from CO concentration of 50, 35, and 0.2 ppm, respectively, will allow us to sense the presence of CO in the ranges, $0.2 < C_{CO} < 35$ ppm, $35 < C_{CO} < 50$ ppm, and $C_{CO} > 50$ ppm. Figure 4 shows such an array and the color changes for $\mathbf{4}\cdot((CH_3)_3CCO_2H)_2$, $\mathbf{2}\cdot(H_2O)_2$, and $\mathbf{5}\cdot(CH_3CO_2H)_2$ derivatives for concentrations of CO of 0, 2, 35, and 50 ppm in air.

Table 6. Summary of the Observed Behavior for VOCs and Gases Tested with All Compounds[a]

	VOCs (ppm)						
solid	acetone	ACN	chloroform	ethanol	formaldehyde	hexane	toluene
$\mathbf{1}\cdot(CH_3CO_2H)_2$	-	4600	-	-	-	-	-
$\mathbf{2}\cdot(CH_3CO_2H)_2$	-	4600	-	-	-	-	-
$\mathbf{2}\cdot(H_2O)_2$	-	4600	-	-	-	-	-
$\mathbf{3}\cdot(CF_3CO_2H)_2$	-	4600	-	-	-	-	-
$\mathbf{4}\cdot((CH_3)_3CCO_2H)_2$	-	4600	-	-	-	-	-
$\mathbf{5}\cdot(CH_3CO_2H)_2$	-	4600	-	-	-	-	-

	gases (ppm)							
solid	water	CO_2	N_2	O_2	Ar	SO_2	NO	NO_2
$\mathbf{1}\cdot(CH_3CO_2H)_2$	-	-	-	-	-	-	8140	2650
$\mathbf{2}\cdot(CH_3CO_2H)_2$	-	-	-	-	-	-	8140	2650
$\mathbf{2}\cdot(H_2O)_2$	-	-	-	-	-	-	814	500
$\mathbf{3}\cdot(CF_3CO_2H)_2$	-	-	-	-	-	-	4070	2650
$\mathbf{4}\cdot((CH_3)_3CCO_2H)_2$	-	-	-	-	-	-	4070	2650
$\mathbf{5}\cdot(CH_3CO_2H)_2$	-	-	-	-	-	-	8140	5000

[a] Both responses are shown: not induced color change (-) and concentrations (in ppm) necessary to induce color changes.

Selectivity. In all cases, the binuclear rhodium complexes studied showed a remarkable selective response to carbon monoxide in air. For instance, no reaction was observed in the presence of CO_2, N_2, O_2, or Ar at very high concentrations (up to 50 000 ppm). Similarly, no color changes were observed in the presence of volatile organic compounds such as acetone, chloroform, ethanol, formaldehyde, hexane, or toluene (up to 30 000 ppm in air). Some color changes to yellow were observed in the presence of acetonitrile vapor, although only at concentrations of 4600 ppm. Studies with other coordinating oxygen-containing gaseous species, such as SO_2, NO, and NO_2, were also carried out. No noticeable color changes were observed on any of the compounds adsorbed on silica beads in the presence of SO_2 (up to 38 000 ppm in air), but NO and NO_2 produced color changes rather similar to those observed in the presence of CO. This reactivity, nevertheless, was only observed at very high concentrations of nitrogen mono- or dioxide. Additionally, whereas the reaction with NO was reversible, the reaction with NO_2 was irreversible. Thus, when the yellow compounds obtained by reaction of the binuclear rhodium derivatives supported on silica with high concentrations of NO were left in NO-free air the solid reverted to purple again, which was not observed for NO_2. All the reactivity and relevant concentration conditions with VOCs and gases tested are summarized in Table 6 where concentrations in which color modulations of the complexes **1**−**5** were observed are shown.

Reversibility of Carbon Monoxide Coordination. Ideal sensing systems not only need to display selectively and sensing features at low concentration but also must be able to show reversible binding with the target analyte. In line with the successful application of the above-mentioned probes, binding of CO in the dinuclear rhodium complexes was found fully reversible. When the yellow solid corresponding to any $\#\cdot(CO)_2$ complex embedded in silica was left in an open air atmosphere, the diffuse reflectance spectra evolve back to the initial corresponding purple complex probe. Although the uptake of CO in the adsorbed compounds occurs in the seconds/minutes time scale, the complete reverse transformation in air from $\#\cdot(CO)_2$ to $\#\cdot\mathbf{L}_2$ takes approximately 15 h at room temperature. Noticeably, the desorption of carbon monoxide from $\#\cdot(CO)_2$ occurs also in two consecutive steps producing initially $\#\cdot(\mathbf{L},CO)$ and the further appearance of the purple dirhodium(II) starting materials, $\#\cdot\mathbf{L}_2$. Figure 5 shows a representative example of the changes observed in the intensity of the band at 400 nm from the diffuse reflectance UV−vis spectrum of the probe from complex $\mathbf{2}\cdot(H_2O)_2$ upon cyclic contact with CO-containing and CO-free air. This cyclic process was repeated at least 10 times without significant degradation of the sensing ability of the material.

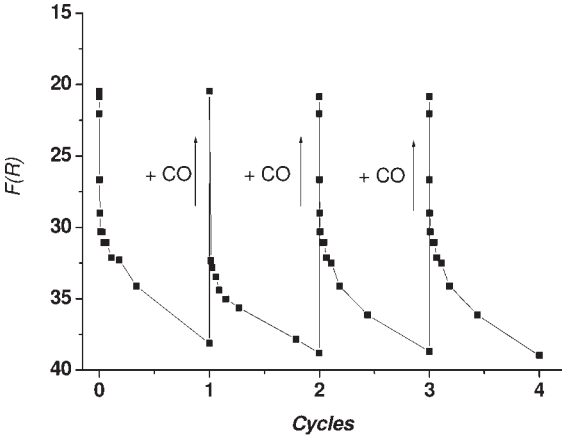

Figure 5. Diffuse reflectance UV−vis spectral response for the band centered at λ = 400 nm for silica beads containing $\mathbf{2}\cdot(CO)_2$ exposed to an air atmosphere. The cycling of the sensor is checked by letting CO-containing air in contact with the sample after full recovery (ca. 15 h) of the starting complex probe.

Moreover, the release of carbon monoxide from the corresponding $\#\cdot(CO)_2$ was followed by thermogravimetry, and in all cases the weight changes correspond to 2 equiv of CO per molecule. Furthermore, no loss of the L ligands from the initial

dx.doi.org/10.1021/ja206251r |J. Am. Chem. Soc. 2011, 133, 15762–15772

#·L_2 probe complexes was observed during the processes, thus indicating that these axial ligands remain adsorbed on the silica beads during all the cycles.

In this respect and to determine the role played by the axial ligand in the reversible CO binding process, the formation and CO release from **2**·$(CO)_2$ using two different starting probe complexes (**2**·$(CH_3CO_2H)_2$ and **2**·$(H_2O)_2$) was monitored thermogravimetrically. Although in both cases two CO molecules are adsorbed/released reversibly, remarkable differences in the release kinetics were found. While for the **2**·$(CO)_2$ derivative obtained from silica bead-supported **2**·$(CH_3CO_2H)_2$ the loss of CO is complete in some hours, the complete CO release from the **2**·$(CO)_2$ derivative obtained from the **2**·$(H_2O)_2$ probe requires ca. two weeks at room temperature.

Kinetico-Mechanistic Studies of the Substitution of CO by L on the Immobilized Compounds. The uptake of carbon monoxide by the immobilized complexes occurs at room temperature in a time scale of minutes, much longer than the practically instant process observed for the systems in solution. Even though the diffusion of gaseous CO into the porous silica beads should play a crucial role in this process, as already established for other immobilized systems,[26,27] no further studies have been carried out for the CO uptake process. The fully reversible character of the process for all adsorbed compounds indicated in Table 1 was confirmed by thermogravimetric and UV−vis analyses (see Scheme 2). As indicated above, the results are especially relevant with respect to the presence of the CO-displaced axial L ligands of the starting material inside the silica beads, which creates the need for a further kinetico-mechanistic investigation of the process.

The release of CO from the #·$(CO)_2$ derivatives obtained from silica immobilized samples of #·L_2 corresponds to the neat weight loss of two CO molecules per dirhodium unit and was studied in detail from a kinetico-mechanistic perspective. The time monitoring at a fixed temperature of this weight loss provided an excellent handle for the measure of the rates of the process, when fitted to a double exponential decay, as corresponds to the intermediate formation of the #·(CO,L) species. Effectively, the weight loss associated to each one of fitted set of two consecutive exponentials is half that of the total decrease, in excellent agreement with the kinetic detection of the #·(CO,L) intermediate complexes (see above and Figure S1 (Supporting Information) for the **5**·$(CO)_2$ complex). The observed first-order character of both consecutive processes can be associated either with a limiting CO dissociative process or with a unimolecular reaction involving the L ligands already attached in an outer-sphere fashion to the dirhodium(II) probe complex.[28] Alternatively, instead of the back coordination of the CO-displaced L ligands, attachment of the available OH groups in the silica beads can also explain such behavior, the L ligands being mere spectators of the process. However, the latter possibility was rejected, as complex **2** (which axial ligands have been extracted via thermal treatment)[29] adsorbed on silica beads was found to be brownish in color, in deep contrast to the purple color of the **2**·L_2 complexes. In the same line, the recycling of the silica beads on CO depletion also reverts to the original spectra for all the adsorbed #·L_2 complexes, a clear indication that the reentry of the original axially bound ligands, L, on the dirhodium compounds is occurring. Consequently all the weight-loss/time traces (Figure S1, Supporting Information) can be fully associated with Scheme 3, where L represents the axial ligands existing in the starting materials.

Scheme 3. Carbon Monoxide Liberation in 2·$(CO)_2$ in Two Consecutive Kinetic Steps, Producing the Regeneration of 2·L_2

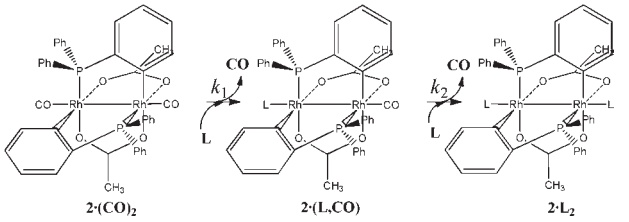

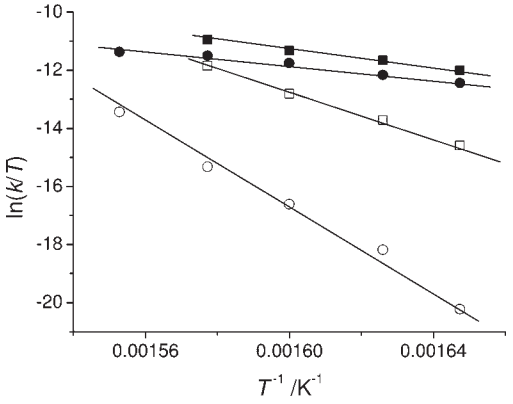

Figure 6. Eyring plot for k_1 (full) and k_2 (empty) rate constants corresponding to CO loss for immobilized compounds **2**·$(CH_3CO_2H)_2$ (squares) and **2**·$(H_2O)_2$ (circles).

The temperature dependence of both k_1 and k_2 rate constants has also been determined by the use of the Eyring equation.[30] Figure 6 shows the plots for two of the starting immobilized compounds studied, **2**·$(CH_3CO_2H)_2$ and **2**·$(H_2O)_2$; the relevant kinetic and thermal activation parameters for these processes on all studied compounds are collected in Table 7.

The very different steric demands of the possible hydrogen bonding interactions for the immobilized complexes, as well as the dramatic change of the σ-donor character of the oxygen donors, are bound to produce important differences between the CO by CH_3CO_2H, CF_3CO_2H, $(CH_3)_3CCO_2H$, or H_2O substitution. As seen in the data collected in Table 7, the thermal activation parameters associated with the faster process (k_1) indicate that for all immobilized compounds the values are surprisingly the same within experimental error, with rather low enthalpies and very negative entropies of activation. These indicate a mechanism with an important degree of ordering during the substitution process with very similar energetics. However, the total recovery of the **2**·$(H_2O)_2$ system is much slower than for the rest of the probes, in good agreement with the differences observed, due to the much lower value of k_2 for the recovery of compound **2**·$(H_2O)_2$.

The only way to come to terms with the surprising homogeneity within the k_1 set of data between such different complexes is by considering that the CO-displaced axial ligand (L) remains still attached via hydrogen bonding interactions to the neighboring bridging carboxylato units of the dirhodium complex. Such interactions have already been described in some Pd(II) XRD data[31] as well as in DFT[32] and mechanistic studies

Table 7. Kinetic and Thermal Activation Parameters for the Processes Indicated in Scheme 3 for Immobilized Complexes #·L_2[a]

compound	$10^3 \times {}^{342}k_1/s^{-1}$	$\Delta H_1^{\ddagger}$/kJ mol^{-1}	$\Delta S_1^{\ddagger}$/J K^{-1} mol^{-1}	$10^4 \times {}^{342}k_2/s^{-1}$	$\Delta H_2^{\ddagger}$/kJ mol^{-1}	$\Delta S_2^{\ddagger}$/J K^{-1} mol^{-1}
$\mathbf{1}\cdot(CH_3CO_2H)_2$	3.6	28 ± 3	−210 ± 8	3.3	60 ± 5	−145 ± 10
$\mathbf{2}\cdot(CH_3CO_2H)_2$	5.3	35 ± 3	−190 ± 11	6.8	100 ± 5	−20 ± 10
$\mathbf{2}\cdot(H_2O)_2$	3.2	30 ± 3	−210 ± 10	0.078	180 ± 5	180 ± 10
$\mathbf{3}\cdot(CF_3CO_2H)_2$	13	33 ± 3	−185 ± 11	16	21 ± 5	−240 ± 10
$\mathbf{4}\cdot((CH_3)_3CCO_2H)_2$	2.4	30 ± 3	−210 ± 10	2.2	85 ± 15	−70 ± 40
$\mathbf{5}\cdot(CH_3CO_2H)_2$	3.5	30 ± 3	−200 ± 11	6.0	75 ± 10	−95 ± 30

[a] k_1 and k_2 were also determined at 334, 352, 361, and 371 K for the evaluation of the thermal activation parameters.

Scheme 4. Mechanism Proposed for CO Liberation in Compounds with Carboxylic Acid As Axial Ligands

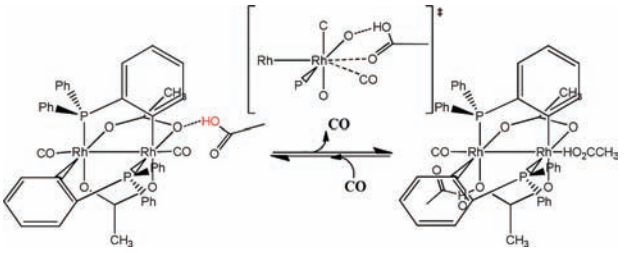

Scheme 5. Possible Outer-Sphere "Solvent-Assisted" Interaction for the $\mathbf{2}\cdot(H_2O)_2$ System

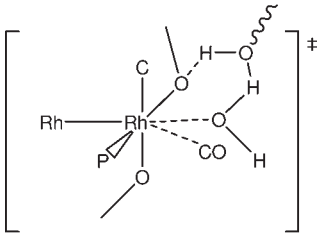

on electrophilic C−H bond activation[13,33] processes assisted by acid. By this attachment, the important differences between the L ligands could be producing, de facto, a rather similar electronics in all cases. Scheme 4 represents a reasonable sequence for such processes exemplified for the $\mathbf{2}\cdot(CH_3CO_2H)_2$ complex. The transition state indicated presents an effective high degree of ordering with little enthalpic demands considering the already "initiated" Rh-carboxylate bonding.

Nevertheless, in the case of decoordinated H_2O arrangement, $\mathbf{2}\cdot(H_2O)_2$, the involvement of the silica OH groups cannot be disregarded, given the existence of a single oxygen donor in the water molecule. An outer-sphere "solvent-assisted" interaction between one of the oxygens of the μ-$CH_3CO_2^-$ group and the H_2O ligand ($\underline{O}$−C(CH$_3$)−$\underline{O}$···H−O···H-$\underline{O}$-H) should be considered as responsible for the similarity with the carboxylic acid systems ($\underline{O}$−C(R)−$\underline{O}$···H−O−C(R)−$\underline{O}$) (Scheme 5).

Examination of the kinetic and thermal activation data for k_2 for the systems studied (Table 7) indicates a general increase of the activation enthalpy accompanied by a decrease of the ordering during the process (less negative or positive activation entropies) with respect to k_1, the exception being for the $\mathbf{3}\cdot(CF_3CO_2H)_2$ complex with very poor σ-donors in its axial positions. Furthermore, the values for $\Delta H^{\ddagger}$ and $\Delta S^{\ddagger}$ are even much more positive for the $\mathbf{2}\cdot(H_2O)_2$ system, thus implying a much more dissociated transition state than for the systems derived from its analogous $\mathbf{2}\cdot(CH_3CO_2H)_2$ probe. Given the fact that the lack of a statistical factor in the value of the rate constants is a clear indication of the electronic transmission via the Rh−Rh bond, already established in equilibrium studies,[11] the better the σ-donor character of the already coordinated first L ligand, the better π-back-donation into the remaining axially bound CO. As a consequence, the process becomes slower, with higher enthalpic demands that promote an important degree of decoordination of CO before the new ligand L can be coordinated to the fairly electron enriched rhodium center. This effect should be very pronounced for L = H_2O and minimal (or even opposite) for L = CF_3CO_2H as effectively observed. Figure 7 shows the $\Delta H^{\ddagger}/\Delta S^{\ddagger}$ compensation plot for all the systems studied, which corroborates the homogeneity of the mechanism operating for all the reactions.

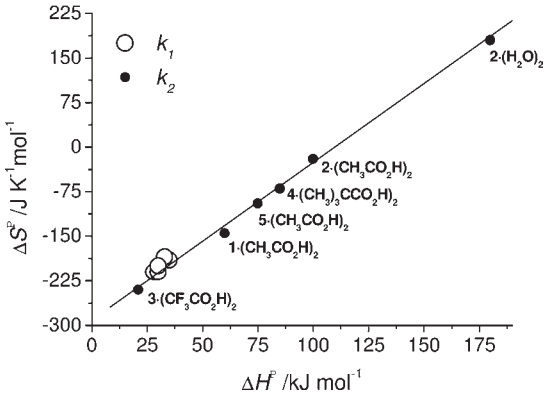

Figure 7. $\Delta H^{\ddagger}/\Delta S^{\ddagger}$ compensation plot for all the systems studied. The values for k_1 cannot be distinguished given its similarity.

CONCLUSIONS

A family of binuclear rhodium compounds of general formula $[Rh_2\{(XC_6H_3)P(XC_6H_4)_2\}_n(O_2CR)_{4-n}]\cdot L_2$ containing one or two, in a head-to-tail arrangement, metalated phosphine ligands and different equatorial and axial ligands have been used as chromogenic chemosensors for CO detection. UV−vis studies were carried out, both in solution and immobilized on silica beads, resulting in hypsochromic shifts. In the case of compounds adsorbed on silica beads in the presence of CO, two different spectra were observed due to the axial coordination of CO groups: orange (one CO in axial position) and yellow (two CO). The crystal structure of $\mathbf{3}\cdot(CHCl_3,CO)$ was solved by

single X-ray diffraction techniques. In all cases the binuclear rhodium complexes studied showed a remarkable low detection limit for CO and a high selective response. From all VOCs and gases tested as possible interferences, the only sensing was observed in the presence of acetonitrile, NO, and NO_2; nevertheless, this only occurs at high concentrations (4600, 4070, and 2650 ppm, respectively). As a special feature, all the complexes tested display a very clear and remarkable color change to the naked eye at concentrations at which CO becomes toxic (i.e., 50−60 ppm). In particular, compound $\mathbf{5\cdot(CH_3CO_2H)_2}$ displays clear color modulations at CO concentrations as low as 0.2 ppm, even allowing the quantification CO in air, based on simple and visual color changes. Binding of CO in these systems was found fully reversible, and the release of carbon monoxide can be monitored by thermogravimetric measurements. The kinetic and thermal activation data obtained for the depletion of CO indicate that the outer-sphere coordination of the L ligands, even in the presence of axially bound CO, is determinant for the easiness and reproducibility of the reversibility of the process. The silica support behaves, especially for L = H_2O, as a noninnocent solvent assisting important interactions that avoid the total removal of the CO-substituted L groups.

EXPERIMENTAL SECTION

General Considerations. Commercially available reagents, $[Rh_2(O_2CCH_3)_4]$, as well as the different phosphines ($P(C_6H_5)_3$, $P(m\text{-}CH_3C_6H_4)_3$) and carboxylic acids (CF_3CO_2H, CH_3CO_2H, $(CH_3)_3CO_2H$), were used as purchased. All solvents were of analytical grade. Column chromatography was carried out on silica gel 60 (230−240 mesh). Solvent mixtures are volume/volume mixtures, unless specified otherwise. All reactions were carried out in oven-dried glassware under an argon atmosphere, although the isolated solids are air-stable. The solvents were degassed before use. All the gases used in this work were generated in situ: carbon monoxide by reaction of sulfuric acid with formic acid; carbon dioxide by adding chloride acid to sodium carbonate; nitrogen monoxide and nitrogen dioxide by oxidation of copper with nitric acid; sulfur dioxide by copper oxidation with sulfuric acid.

Compounds. *[Rh$_2${(XC$_6$H$_3$)P(XC$_6$H$_4$)$_2$}$_2$(O$_2$CR)$_2$]·L$_2$.* $[Rh_2\{(XC_6H_3)P(XC_6H_4)_2\}_2(O_2CR)_2]\cdot L_2$ complexes, $\mathbf{2\cdot(CH_3CO_2H)_2}$ and $\mathbf{5\cdot(CH_3CO_2H)_2}$, were obtained by refluxing the corresponding phosphine with $[Rh_2(O_2CCH_3)_4]$ in toluene:acetic acid media (3:1) under argon atmosphere as described in the literature.[15,34,35] For these compounds with two cyclometalated phosphines, the molar ratio phosphine:dirhodium(II) tetraacetate was 2:1. These compounds containing two *ortho*-metalated aryl phosphines and two carboxylates as bridging ligands show fast and quantitative interchange of both carboxylate ligands by other bridging ligands,[36] which facilitates the interchange with other carboxylates. Thus, other derivatives with the same *ortho*-metalated dirhodium(II) skeleton can be easily obtained (see below).

Compounds of general formula $[Rh_2\{(XC_6H_3)P(XC_6H_4)_2\}_2(O_2CR)_2]\cdot L_2$, $\mathbf{3\cdot(CF_3CO_2H)_2}$, and $\mathbf{4\cdot((CH_3)_3CCO_2H)_2}$ were obtained by stirring the starting product, $\mathbf{2\cdot(CH_3CO_2H)_2}$, in the presence of an excess of the substituting carboxylic acid (trifluoroacetic and pivalic acid, respectively) in chloroform solution. The mixture was then heated under reduced pressure to dryness. The procedure was repeated until the complete interchange was produced (5−6 times). The excess of the acid was then eliminated by column chromatography (CH_2Cl_2:Hexane 2:1).

$[Rh_2\{(C_6H_4)P(C_6H_5)_2\}_2(O_2CCH_3)_2]\cdot(H_2O)_2$, $\mathbf{2\cdot(H_2O)_2}$, was obtained by stirring $\mathbf{2\cdot(CH_3CO_2H)_2}$ in the presence of an excess of sodium carbonate in acetone. In this procedure, the water contained in the acetone is the origin of the substituting axial ligand. The resulting compounds were obtained after removal of the solvent under reduced pressure.

[Rh$_2${(XC$_6$H$_3$)P(XC$_6$H$_4$)$_2$}(O$_2$CR)$_3$]·L$_2$. $[Rh_2\{(C_6H_4)P(C_6H_5)_2\}(O_2CCH_3)_3]\cdot(CH_3CO_2H)_2$ complex, $\mathbf{1\cdot(CH_3CO_2H)_2}$, was obtained following the same synthetic procedure as used for compounds with general formula $[Rh_2\{(XC_6H_3)P(XC_6H_4)_2\}_2(O_2CR)_2]\cdot L_2$ but using a phosphine:dirhodium(II) tetraacetate molar ratio of 0.9:1.

Silica Gel Immobilization of the Dirhodium(II) Complexes. Each binuclear rhodium compound was dissolved in a minimum volume of $CHCl_3$. An excess of silica (230−240 mesh, weight ratio 2−10-fold) was added to the colored solution, and the resulting mixture was stirred at room temperature for five minutes. After removal of the solvent on a rotary evaporator, the solid was dried in an oven at 343 K during at least two days prior to its use. A careful weight control of the samples was carried out, indicating that the effective final weight corresponds to the mass of silica plus the mass of the $\mathbf{\#\cdot L_2}$ complex and that no evolution from the silica beads of the axially bound ligands, L, has occurred under the working conditions.

Instrumentation. Infrared spectra were recorded at room temperature on a JASCO FT-IR 460 Plus spectrometer. UV−vis spectra were recorded using a Jasco V-650 spectrophotometer equipped with a diffuse reflectance Sphere (model ISV-722 Sphere) for measurements on solids. In the latter case, measurements were conducted at room temperature over a wavelength range of 350−800 nm with a wavelength step of 1 nm. The reflectance data were transformed using Kubelka−Munk function $[F(R)]$,[37] where R is the fraction of incident light reflected by the sample.

$$F(R) = \frac{(1-R)^2}{2R}$$

For kinetic studies, CO loss was monitored via thermogravimetric analyses carried out on a TGA/SDTA 851e Mettler Toledo balance, set at a fixed temperature, using nitrogen as purge gas. The fitting of the weight changes versus time to a double exponential decay with identical amplitudes was carried out by the standard software packages available. Carbon monoxide concentrations were measured by an ambient carbon monoxide analyzer (Testo 315−2 model 0632 0317), properly validated with a calibration certificate issued by Spanish Certification Entity (ENAC).

X-ray data collection was performed on a Bruker Kappa CCD diffractometer using graphite monochromated Mo Kα radiation (λ = 0.71073 Å) at 293 K. Data reduction and cell refinements were performed with HKL DENZO and SCALEPACK programs.[23] Crystal structures were solved by direct methods with the aid of successive difference Fourier maps and were refined using the SHELXTL 6.1 software package.[38] All non-hydrogen atoms were refined anisotropically. High residual electronic density was found around the CF_3 groups in the trifluoroacetate ligands, and very anisotropic thermal ellipsoids were obtained for fluorine atoms. Hence, a disordered model for CF_3 groups was applied using a riding model refinement and constraining the occupancy to one for those groups bonded to the same carbon atom in both acetate ligands. The hydrogen atoms were assigned to ideal positions and refined using a riding model. The details of the data collection, cell dimensions, and structure refinement are given in the Supporting Information. Full crystallographic data have been deposited in the Cambridge Crystallographic Data Centre with the number CCDC 820952.

RGB values were analyzed using Adobe Photoshop Elements 7.0 software.

ASSOCIATED CONTENT

Supporting Information. Crystallographic data and structure refinement of $[Rh_2[(C_6H_4)P(C_6H_5)_2]_2(O_2CCH_3)_2]\cdot(CO)$ ($\mathbf{3\cdot CO}$). Selected geometric data for $[Rh_2[(C_6H_4)P(C_6H_5)_2]_2(O_2CCH_3)_2]\cdot(CO)$ ($\mathbf{3\cdot CO}$) at 293 K. Weight loss of a sample of

$5\cdot(CO)_2$ with time at 50 °C. This material is available free of charge via the Internet at http://pubs.acs.org.

AUTHOR INFORMATION

Corresponding Author
rmaez@qim.upv.es; manel.martinez@qi.ub.es.

ACKNOWLEDGMENT

The authors wish to express their gratitude to the Spanish Ministerio de Ciencia y e Innovación (projects MAT2009-14564-C04-01 and CTQ2009-14443-C02-02) and Generalitat Valenciana (project PROMETEO/2009/016) for their support. MEM is grateful to the Spanish Ministerio de Ciencia e Innovación for an FPU grant.

REFERENCES

(1) (a) Wattel, F.; Favory, R.; Lancel, S.; Neviere, R.; Mathieu, D. *Bull. Acad. Natl. Med.* **2006**, *190*, 1961–1975. (b) McGrath, J. J. *Carbon Monoxide*, 2nd ed.; Salem, H., Katz, S. A., Eds.; CRC, Boca Raton, **2006**; p 695. (c) Wilkinson, L. J.; Waring, R. H.; Steventon, G. B.; Mitchell, S. C. *Molecules of death. Carbon monoxide-the silent killer*, 2nd ed.; Imperial College Press, London, 2007.

(2) http://emedicine.medscape.com/article/1009092-overview (accessed May 25, 2011).

(3) (a) Claireaux, G.; Thomas, S.; Fievet, B.; Motais, R. *Respir. Physiol.* **1988**, *74*, 91–98. (b) Marsh, M. G.; Marino, G.; Pucci, P.; Ferranti, P.; Malorni, A.; Kaeda, J.; Marsh, J.; Luzzatto, L. *Hemoglobin* **1991**, *15*, 43–51.

(4) Benzon, H. T.; Brunner, E. A. *JAMA* **1978**, *240*, 1955–1964.

(5) Wang, B.; Zhao, Y. D.; Hu, L. M.; Cao, J. S.; Gao, F. L.; Liu, Y.; Wang, L. J. *Chin. Sci. Bull.* **2010**, *55* (3), 228–232.

(6) Itou, M.; Araki, Y.; Ito, O.; Kido, H. *Inorg. Chem.* **2006**, *45*, 6114–6116.

(7) Paul, S.; Amalraj, F.; Radhakrishnana, S. *Synt. Math.* **2009**, *159*, 1019–1061.

(8) Benito-Garagorri, D.; Puchberger, M.; Mereiter, K.; Kirchner, K. *Angew. Chem., Int. Ed.* **2008**, *47*, 9142–9145.

(9) Giulino, A.; Gupta, T.; Altman, M.; Lo Schiavo, S.; Mineo, P. G.; Fragalà, I. L.; Evmenenko, G.; Dutta, P.; Van der Boom, M. E. *Chem. Commun* **2008**, 2900–2902.

(10) See for instance: (a) Climent, E.; Marcos, M. D.; Martínez-Máñez, R.; Sancenón, F.; Soto, J.; Rurack, K.; Amorós, P. *Angew. Chem., Int. Ed.* **2009**, *48*, 8519–8522. (b) Climent, E.; Bernardos, A.; Martínez-Máñez, R.; Maquieira, A.; Marcos, M. D.; Pastor-Navarro, N.; Puchades, R.; Sancenón, F.; Soto, J.; Amorós, P. *J. Am. Chem. Soc.* **2009**, *131*, 14075–14080. (c) Comes, M.; Aznar, E.; Moragues, M.; Marcos, M. D.; Martínez-Máñez, R.; Sancenón, F.; Soto, J.; Villaescusa, L. A.; Gil, L.; Amorós, P. *Chem.—Eur. J.* **2009**, *15*, 9024–9033. (d) Ábalos, T.; Royo, S.; Martínez-Máñez, R.; Sancenón, F.; Soto, J.; Costero, A. M.; Gil, S.; Parra, M. *New J. Chem.* **2009**, *33*, 1641–1645. (e) Aznar, E.; Coll, C.; Marcos, M. D.; Martínez-Máñez, R.; Sancenón, F.; Soto, J.; Amorós, P.; Cano, J.; Ruiz, E. *Chem.—Eur. J.* **2009**, *15*, 6877–6888. (f) Climent, E.; Calero, P.; Marcos, M. D.; Martínez-Máñez, R.; Sancenón, F.; Soto, J. *Chem.—Eur. J.* **2009**, *15*, 1816–1820.

(11) Hirva, P.; Esteban, J.; Lahuerta, P.; Pérez-Prieto, J. *Inorg. Chem.* **2007**, *46*, 2619–2626.

(12) Esteban, J.; Ros-Lis, J. V.; Martínez-Mañez, R.; Marcos, M. D.; Moragues, M.; Soto, J.; Sancenón, F. *Angew. Chem., Int. Ed.* **2010**, *49*, 4934–4937.

(13) Estevan, F.; González, G.; Lahuerta, P.; Martínez, M.; Peris, E.; van Eldik., R. *J. Chem. Soc., Dalton Trans.* **1996**, 1045–1050.

(14) Esteban, J.; Hirva, P.; Lahuerta, P.; Martínez, M. *Inorg. Chem.* **2006**, *45*, 8776–8784.

(15) Hirva, P.; Lahuerta, P.; Pérez-Prieto, J. *Theor. Chem.* **2005**, *113*, 63–68.

(16) (a) Estevan, F.; Lahuerta, P.; Pérez-Prieto, J.; Pereira, I.; Stiriba, S. E. *Organometallics* **1998**, *17*, 3442–3447. (b) Estevan, F.; Lahuerta, P.; Pérez-Prieto, J.; Sanaú, M.; Stiriba, S. E.; Úbeda, M. A. *Organometallics* **1997**, *16*, 880–886. (c) Barberis, M.; Lahuerta, P.; Pérez-Prieto, J.; Sanaú, M. *Chem. Commun.* **2001**, 439–440. (d) Barberis, M.; Pérez-Prieto, J.; Stiriba, S. E.; Lahuerta, P. *Org. Lett.* **2001**, *3*, 3317–3319. (e) Estevan, F.; Herbst, K.; Lahuerta, P.; Barberis, M.; Pérez-Prieto, J. *Organometallics* **2001**, *20*, 950–957.

(17) Drago, R. S.; Tanner, S. P.; Ritchman, R. M.; Long, J. R. *J. Am. Chem. Soc.* **1979**, *101*, 2897–2903.

(18) González, G.; Martínez, M.; Estevan, F.; García-Herbosa, G.; Lahuerta, P.; Peris, E.; Ubeda, M.; Diaz, M. R.; Garcia-Granda, S.; Tejerina, B. *New J. Chem.* **1996**, *20*, 83–94.

(19) Esteban, J. *PhD Thesis* 2006, Universitat de València.

(20) Chakravarty, A. R.; Cotton, F. A.; Tocher, D. A.; Tocher, J. H. *Organometallics* **1985**, *4*, 8–13.

(21) (a) Barcel, F.; Cotton, F. A.; Lahuerta, P.; Llusar, R.; Sanaú, M.; Schwotzer, W.; Úbeda, M. A. *Organometallics* **1986**, *5*, 808–811. (b) Barcel, F.; Cotton, F. A.; Lahuerta, P.; Sanaú, M.; Schwotzer, W.; Úbeda, M. A. *Organometallics* **1987**, *6*, 1105–1110. (c) Cotton, F. A.; Dunbar, K. R.; Verbruggen, M. G. *J. Am. Chem. Soc.* **1987**, *109*, 5498–5506. (d) Cotton, F. A.; Dunbar, K. R. *J. Am. Chem. Soc.* **1987**, *109*, 3142–3143. (e) Cotton, F. A.; Dunbar, K. R.; Eagle, C. T. *Inorg. Chem.* **1987**, *26*, 4127–4130. (f) Lahuerta, P.; Paya, J.; Peris, E.; Pelinghelli, M. A.; Tiripicchio, A. *J. Organomet. Chem.* **1989**, *373*, C5–C7. (g) Morrison, E. C.; Tocher, D. A. *Inorg. Chim. Acta* **1989**, *156*, 99–105. (h) Morrison, E. C.; Tocher, D. A. *Inorg. Chim. Acta* **1989**, *157*, 139–140. (i) Lahuerta, P.; Payá, J.; Peris, E.; Aguirre, A. S.; García-Granda, A.; Gómez-Beltrán, F. *Inorg. Chim. Acta* **1992**, *192*, 43–49. (j) Lahuerta, P.; Payá, J.; Solans, X.; Úbeda, M. A. *Inorg. Chem.* **1992**, *31*, 385–391. (k) Lahuerta, P.; Peris, E. *Inorg. Chem.* **1992**, *31*, 4547–4551. (l) Borrachero, M. V.; Estevan, F.; Lahuerta, P.; Payá, J.; Peris, E. *Polyhedron* **1993**, *12*, 1715–1717. (m) Estevan, F.; Lahuerta, P.; Latorre, J.; Peris, E.; García-Granda, S.; Gómez-Beltrán, F.; Aguirre, A.; Salvad, M. A. *J. Chem. Soc., Dalton Trans.* **1993**, 1681–1688. (n) Lahuerta, P.; Úbeda, M. A.; Payá, J.; García-Granda, S.; Gómez-Beltrán, F.; Anillo, A. *Inorg. Chim. Acta* **1993**, *205*, 91. (o) Lahuerta, P.; Latorre, J.; Peris, E.; Sanaú, M.; Ubeda, M. A.; Garcia-Granda, S. *J. Organomet. Chem.* **1993**, *445*, C10–12. (p) Pruchnik, F. P.; Starosta, R.; Lis, T.; Lahuerta, P. *J. Organomet. Chem.* **1998**, *568*, 177–183. (q) Pruchnik, F. P.; Starosta, R.; Smolenski, P.; Shestakova, E.; Lahuerta, P. *Organometallics* **1998**, *17*, 3684–3689.

(22) (a) Taber, D. F.; Malcolm, S. C.; Bieger, K.; Lahuerta, P.; Sanaú, M.; Stiriba, S. E.; Pérez-Prieto, J.; Monge, M. A. *J. Am. Chem. Soc.* **1999**, *121*, 860–861. (b) Lahuerta, P.; Martínez-Mañez, R.; Payá, J.; Peris, E. *Inorg. Chim. Acta* **1990**, *173*, 99–105. (c) Lahuerta, P.; Payá, J.; Pellinghelli, M. A.; Tiripicchio, A. *Inorg. Chem.* **1992**, *31*, 1224–1232.

(23) Otwinowski, Z.; Minor, W. *Methods Enzymol.* **1997**, *276*, 307–326.

(24) The crystal structure of $[Rh_2[(C_6H_4)P(C_6H_5)_2]_2(O_2CCH_3)_2]\cdot(CO)$ (**3·CO**) has been deposited at the Cambridge Crystallographic Data Centre and allocated the deposition number CCDC 820952.

(25) Kou, X.; Rasika Dias, H. V. *Dalton Trans.* **2009**, 7529–7536.

(26) Basallote, M. G.; Bozoglián, F.; Fernandez-Trujillo, M. J.; Martínez, M. *New J. Chem.* **2007**, *32*, 264–272.

(27) Basallote, M. G.; Blanco, E.; Blázquez, M.; Fernández-Trujillo, M. J.; Litrán, R.; Máñez, M. A.; Ramírez del Solar, M. *Chem. Mater.* **2003**, *15*, 2525–2532.

(28) Espenson, J. H. *Chemical Kinetics and Reaction Mechanisms*; McGraw-Hill: New York, 1981.

(29) A sample of silica containing the complex was heated at a rate of 5° per minute until a weight loss equivalent to the two L ligands is observed. Alternatively, when stirring a suspension of the prepared silica-adsorbed sample in chloroform at 70 °C for prolonged periods, followed by reduced pressure drying, a sample of axially free dirhodium complex was also produced.

(30) Tobe, M. L.; Burgess, J. *Inorganic Reaction Mechanisms*; Longman: U.K., 1999.

(31) Albert, J.; Andrea, L.; Bautista, J.; Gonzalez, A.; Granell, J.; Font-Bardia, M.; Calvet, T. *Organometallics* **2008**, *27*, 5108–5117.
(32) Aullón, G.; Chat, R.; Favier, I.; Font-Bardía, M.; Gómez, M.; Granell, J.; Martínez, M.; Solans, X. *Dalton Trans* **2009**, 8292–8300.
(33) (a) Gómez, M.; Granell, J.; Martínez, M. *Eur. J. Inorg. Chem.* **2000**, 217–224. (b) Gómez, M.; Granell, J.; Martínez, M. *J. Chem. Soc., Dalton Trans.* **1998**, 37–44. (c) González, G.; Lahuerta, P.; Martínez, M.; Peris, E.; Sanau, M. *J. Chem. Soc., Dalton Trans.* **1994**, 545–550.
(34) Esteban, J.; Esteban, F.; Sanau, M. *Inorg. Chim. Acta* **2009**, *362*, 1179–1184.
(35) Esteban, J.; Esteban, F.; Sanau, M. *Inorg. Chim. Acta* **2008**, *361*, 1274–1280.
(36) Lahuerta, P.; Peris, E. *Inorg. Chem.* **1992**, *31*, 4547–4551.
(37) Zinchuk, A. V.; Hancock, B. C.; Shalaev, E. Y.; Reddy, R. D.; Govindarajan, R.; Novak, E. *Eur. J. Pharm. Biopharm.* **2005**, *61*, 158–170.
(38) Sheldrick, G. M. *SHELXTL*, v. 5.1; Bruker AXS, Inc. ed.: Madison, WI, 2000.